Heliyon 6 (2020) e04236

Contents lists available at ScienceDirect

Heliyon

www.elsevier.com/locate/heliyon

Research article

Buckling of thin skew isotropic plate resting on Pasternak elastic foundation using extended Kantorovich method

Ahmed Hassan Ahmed Hassan *, Naci Kurgan

Mechanical Engineering Department, Engineering Faculty, Ondokuz Mayis University, 55139 Atakum, Samsun, Turkey

ARTICLE INFO

Keywords:
Civil engineering
Mechanical engineering
Structural engineering
Foundation Engineering
Structural Analysis
Structural Mechanics
Extended Kantorovich method (EKM)
Thin plate
Skew plate
Buckling
Pasternak elastic foundation
Galerkin's weighted residual method

ABSTRACT

The extended Kantorovich method (EKM) is implemented to numerically solve the elastic buckling problem of thin skew (parallelogram) isotropic plate under in-plane loading resting on the Pasternak elastic foundation. EKM has never been applied to this problem before. Investigation of the EKM accuracy and convergence is conducted. Formulations are based on classical plate theory (CPT). Stability equations and boundary conditions terms are derived from the principle of the minimum total potential energy using the variational calculus expressed in an oblique coordinate system. The resulting two sets of ordinary differential equations are solved numerically using the Chebfun package in MATLAB software. In-plane compression and shear loads are considered along with various boundary conditions and aspect ratios. Results are compared to the analytical and numerical solutions found in the literature, and to the finite element solutions obtained using ANSYS software. The effects of the skew angle, stiffness of elastic foundation, and aspect ratio on the buckling load are also investigated. For plates with zero skew angle, i.e. rectangular plates, with various boundary conditions and aspect ratios under uniaxial and biaxial loading resting on elastic foundation, the single-term EKM is found accurate. However, more terms are needed as the skew angle gets bigger. The multi-term EKM is found accurate in the analysis of rectangular and skew plates with various boundary conditions and aspect ratios under uniaxial, biaxial, and shear loading resting on elastic foundation. Using EKM in buckling analysis of thin skew plates is found simple, accurate, and rapid to converge.

1. Introduction

Relatively thin structures with a wide flat planar surface are normally called plates (Reddy, 2006). The plate is one of the main modeling elements used in analyzing the engineering structures. Many theories have been proposed to model plates based on the simplifications gained from the relative smallness of their thickness. The simplest one is the classical plate theory (CPT), developed in 1881 (Ventsel and Krauthammer, 2001), which describes thinner plates. Many engineering applications require plates in skew geometry (Srinivasa et al., 2018), e.g. the tail-fin and swept wings of airplanes (MonroeAerospacecom, 2019). In the field of mechanics of material, the study of plates consists of three main analyses: bending, buckling, and vibration analysis (Reddy, 2006). When a flat plate falls under compression in-plane loads at its edges or thermal loads with constrained edges, buckling and post-buckling analysis have to be conducted to ensure correct prediction of the plate's behavior. Numerous methods are applied in the buckling analysis of plates. In general, they can be divided into two major categories; stochastic and deterministic methods. Stochastic buckling analysis includes the uncertainty in material properties, loads, and geometry (e.g. Gadade et al., 2020). Deterministic methods are the common ones in buckling analysis of thin plates. Among the most important of them which are frequently implemented in buckling analysis are Ritz method (e.g. Kitipornchai et al., 2017), differential quadrature methods (e.g. Wu et al., 2017) and finite element method (e.g. Manickam et al., 2018). Another method that getting increasing attention in this field of analysis is the extended Kantorovich method (EKM).

EKM was introduced by Kerr (1968) as a method to solve partial differential equations (PDE) by reducing the problem to a set of ordinary differential equations (ODE) which are then solved iteratively one at a time starting from an arbitrary set of trail functions. Unlike Galerkin and Ritz methods, EKM has less dependency on the assumed trail functions. Implementing EKM in the analysis of plates started early by the author of the EKM by solving the plate bending problem (Kerr and Alexander, 1968), and vibration and buckling problems (Kerr, 1969). Then,

* Corresponding author.
E-mail addresses: 15210457@stu.omu.edu.tr (A.H.A. Hassan), naci.kurgan@omu.edu.tr (N. Kurgan).

https://doi.org/10.1016/j.heliyon.2020.e04236
Received 6 April 2020; Received in revised form 4 May 2020; Accepted 15 June 2020

EKM has been implemented in many studies of plate problems. Singhatanadgid and Singhanart (2019) presented a review of those studies.

EKM has been implemented by a few researchers in the bending analysis of the skew plates. Following is a listing of those articles. Joodaky and co-authors obtained closed-form solution for bending of clamped thin isotropic skew plate (Kargarnovin et al., 2010), clamped thin skew FGM plate (Joodaky et al., 2012) and thin FGM skew plate resting on elastic foundations (Joodaky et al., 2013; Joodaky and Joodaky, 2015). Hassan and Kurgan (2020) compared the single-term EKM to the multi-term EKM for the bending analysis of thin skew plates. They showed the necessity of using the multi-term EKM to obtain accurate results throughout the area of the thin skew plate. Rajabi and Mohammadimehr (2019) implemented multi-term EKM in the bending analysis of thin micro-sandwich skew plates resting on elastic foundation. Shufrin et al. (2010) applied the multi-term EKM on the extended problem that considers the general trapezoidal plates which include the skew plates as a special case.

Many articles present the use of EKM in both numerical (e.g. Grimm and Gerdeen, 1975; Eisenberger and Alexandrov, 2003; Shufrin and Eisenberger, 2005a,b, 2006, 2007; Yuan and Jin, 1998) and semi-analytical (e.g. Chen, 1972; Yu and Zhang, 1986; Zhang and Yu, 1988; Xie and Elishakoff, 2000) buckling analysis of various isotropic plate problems. Fewer studies implemented EKM to investigate buckling of laminated plates (e.g. Ungbhakorn and Singhatanadgid, 2006; Shufrin et al., 2008a,b; Singhatanadgid and Jommalai, 2016; Lopatin and Morozov, 2013) and orthotropic plates (e.g. Eisenberger and Shufrin, 2009; Shufrin et al., 2009). All those studies considered rectangular plates, except (e.g. Yu and Zhang, 1986; Zhang and Yu, 1988) in which annular plates were considered. However, the buckling of skew plates has never been investigated using neither the single-term nor the multi-term EKM but other methods, including Galerkin's method (e.g. Saadatpour et al., 1998), Rayleigh-Ritz method (e.g. Kitipornchai et al., 1993), element free Galerkin method (e.g. Jaberzadeh et al., 2013), finite element method (FEM) (e.g. Jaunky et al., 1995), double Fourier method (e.g. Kennedy and Prabhakara, 1978), Lagrangian multiplier method (e.g. Mizusawa et al., 1980), and recently finite strip method (e.g. Shahrestani et al., 2018) and differential quadrature method (DQM) (e.g. Wang and Yuan, 2018).

An important problem to consider when analyzing plates is the effect of elastic foundations on the behavior of the plate. The simplest elastic foundation is the Winkler model, which treats the foundation as a series of separated springs without coupling effects between each other. Pasternak model adds a shear layer to the Winkler model as a second parameter. The Pasternak model is widely used to describe the mechanical interactions between structure and foundation (Mahmoudi et al., 2017). A more complicated elastic foundation model is Kerr's model, which adds a third parameter as an additional shear layer (Shahsavari et al., 2018).

To the best of the authors' knowledge, the buckling of skew isotropic plates has not been investigated using EKM yet. Implementing EKM to investigate the buckling of skew plates is presented here for the first time. Stability equations and boundary conditions are derived using the principle of minimum total potential energy. This article aims to assess the accuracy and convergence of the EKM as a numerical solution method to the problem of buckling analysis of thin skew plates under in-plane uniform compression or shear loading resting on the Pasternak elastic foundation and compare the results with those obtained using other methods.

2. Theoretical formulation

Consider the skew plate shown in Fig. 1, having a skew angle (ϕ), under uniform in-plane loads each acts parallel to one of the edges of the plate, as shown in Fig. 2, resting on the Pasternak elastic foundation shown in Fig. 3. Firstly, the basic terms and equations in the rectangular coordinate system are introduced, then the oblique coordinate system is introduced and the equation of the total potential energy in rectangular coordinate $(x-y)$ system is transformed to the oblique coordinate system $(\xi-\eta)$, from which the stability equations and boundary conditions will be later derived.

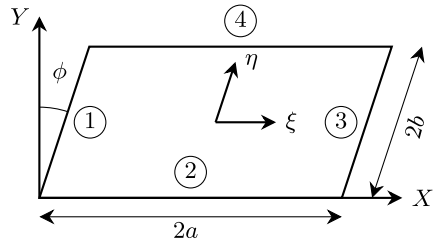

Fig. 1. Coordinate systems convention and edge labeling.

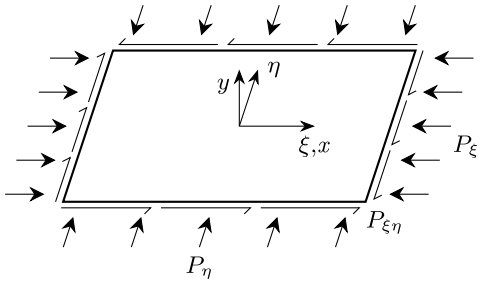

Fig. 2. In-plane loading on edges.

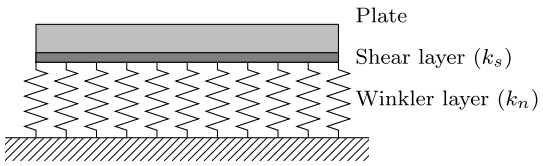

Fig. 3. Pasternak elastic foundation model.

2.1. Basic equations and terms

Based on the classical plate theory CPT, the total potential energy (e_p) of a thin rectangular plate having flexural rigidity (D), Poisson's ratio (ν), and dimensions $2a\times 2b$ experiencing in-plane axial (N_x, N_y) and shear (N_{xy}) stress resultants resting on the Pasternak elastic foundation having normal and shear stiffness (k_n, k_p), is a functional of the function $w(x,y)$, given as

$$e_p(w(x,y)) = \tag{1}$$

$$\frac{D}{2}\iint\left[w_{,xx}^2+w_{,yy}^2+2\nu w_{,xx}w_{,yy}+2(1-\nu)w_{,xy}^2\right]dxdy$$

$$+\frac{1}{2}\iint\left[k_n w^2+k_p\left(w_{,x}^2+w_{,y}^2\right)\right]dxdy$$

$$-\frac{1}{2}\iint\left[N_x w_{,x}^2+N_y w_{,y}^2+2N_{xy}w_{,x}w_{,y}\right]dxdy$$

where $w(x,y)$ is the lateral deflection at any point (x,y) on the physical neutral plane which is the mid-plane for the case of isotropic homogeneous plates. The subscripts after commas indicate the derivatives in the stated directions. The flexural rigidity of the plate (D), also called bending stiffness in some references, is given by

$$D=\frac{h^3E}{12\left(1-\nu^2\right)} \tag{2}$$

where (E) is the Young's modulus of the plate, (ν) is the Poisson's ratio and (h) is thickness of the plate.

Stress resultants (N_x, N_y, N_{xy}) are in units of load per unit length (N/m). The negative sign of the stress resultants indicates that they are compression resultants. For the plates with constant thickness (h), stress resultants are given by

$$\begin{bmatrix} N_x & N_y & N_{xy} \end{bmatrix} = \int_{-h/2}^{h/2} \begin{bmatrix} \sigma_x & \sigma_y & \sigma_{xy} \end{bmatrix} dz \tag{3}$$

where σ's are the normal and shear in-plane stress components. For the case of in-plane uniformly distributed loads, the stress components σ's are given by

$$\begin{bmatrix} \sigma_x & \sigma_y & \sigma_{xy} \end{bmatrix} = \frac{1}{h} \begin{bmatrix} P_x & P_y & P_{xy} \end{bmatrix} \tag{4}$$

where P's are the in-plane uniformly distributed loads in units of load per unit length (N/m). Comparing Eq. (3) with Eq. (4) shows that the stress resultants (N_x, N_y, N_{xy}) are equal to the uniformly distributed loads (P_x, P_y, P_{xy}).

The Pasternak elastic foundation model, shown in Fig. 3, treats the bond between a plate and its foundation as two stacked layers. The first consists of closely spaced independent linear springs having only out-of-plane extension stiffness coefficient (k_n) in units of load over the unit area for the unit lateral deflection of that area $(N/m^2/m)$, while the second layer has only shear stiffness coefficient (k_p) in units of load over unit in-plane shearing (N/m). If only the former stiffness (k_n) is considered then the model reduces to be Winkler foundation. Often, k_n and k_p are expressed in nondimensional form as k_n^* and k_p^* given by

$$k_n^* = \frac{k_n a^4}{100D}; \quad k_p^* = \frac{k_p a^2}{100D} \tag{5}$$

where (a) is the half of length of the plate.

2.2. Oblique coordinate system and transformations

Considering coordinate systems shown in Fig. 1, the relation between oblique $(\xi - \eta)$ and Cartesian $(x - y)$ coordinate systems is a function of the skew angle ϕ as

$$\begin{bmatrix} x \\ y \end{bmatrix} = \begin{bmatrix} 1 & s \\ 0 & c \end{bmatrix} \begin{bmatrix} \xi \\ \eta \end{bmatrix} \tag{6}$$

where $c = \cos\phi$; and $s = \sin\phi$. By using Eq. (6), any function in the Cartesian coordinates and its derivatives can be transformed to the corresponding function and derivatives in the oblique coordinate system. The angle of the oblique coordinate system is chosen to be the same angle of the considered skew plate, such that each edge of the plate be parallel to one of the axes.

Lateral deflection $w(x, y)$ terms in the potential energy equation of the rectangular plate given in Eq. (1) are transformed into the oblique coordinates $(\xi - \eta)$ as

$$\begin{aligned} w(x,y) &\to w(\xi,\eta) & w_{,y} &\to c^{-1}\left(-s\, w_{,\xi} + w_{,\eta}\right) \\ w_{,x} &\to w_{,\xi} & w_{,xy} &\to c^{-1}\left(-s\, w_{,\xi\xi} + w_{,\eta\xi}\right) \\ w_{,xx} &\to w_{,\xi\xi} & w_{,yy} &\to c^{-2}\left(s^2\, w_{,\xi\xi} - 2s\, w_{,\xi\eta} + w_{,\eta\eta}\right) \\ \int dx &\to \int d\xi & \int dy &\to \int c\, d\eta \end{aligned} \tag{7}$$

Transformation of the in-plane stress components illustrated by Wang and Yuan (2018) along with Eq. (3) and Eq. (4) reveal the transformation of the stress resultants as

$$\begin{aligned} N_x &= c^{-1}\left(N_\xi + 2s\, N_{\xi\eta} + s^2\, N_\eta\right) \\ N_y &= c\, N_\eta \\ N_{xy} &= N_{\xi\eta} + s\, N_\eta \end{aligned} \tag{8}$$

Furthermore, using again Eq. (3) and Eq. (4) gives that the stress resultants in the oblique coordinate system equal to the uniformly distributed loads, i.e.

$$\begin{bmatrix} P_\xi & P_\eta & P_{\xi\eta} \end{bmatrix} = \begin{bmatrix} N_\xi & N_\eta & N_{\xi\eta} \end{bmatrix} \tag{9}$$

At last, substituting of the transformations presented in Eq. (7), Eq. (8) and Eq. (9) into Eq. (1) gives the potential energy functional of the function $w(\xi, \eta)$, as

$$\begin{aligned} e_p(w(\xi,\eta)) = & \\ & \frac{D}{2c^3} \iint \Big[w_{,\xi\xi}^2 + w_{,\eta\eta}^2 + 2R_1 w_{,\xi\xi} w_{,\eta\eta} \\ & \qquad - 4s w_{,\xi\eta}\left(w_{,\xi\xi} + w_{,\eta\eta}\right) + 2R_2 w_{,\xi\eta}^2 \Big] d\xi d\eta \\ & + \frac{1}{2} \iint \left[k_n w^2 + \frac{k_p}{c}\left(w_{,\xi}^2 + w_{,\eta}^2 - 2s w_{,\xi} w_{,\eta}\right) \right] d\xi d\eta \\ & - \frac{1}{2} \iint \left[P_\xi w_{,\xi}^2 + P_\eta w_{,\eta}^2 + 2P_{\xi\eta} w_{,\xi} w_{,\eta} \right] d\xi d\eta \end{aligned} \tag{10}$$

where R_1 and R_2 are constants given as

$$R_1 = s^2 + \nu c^2 \qquad R_2 = R_1 - 1$$

2.3. Non-dimensional buckling factor

Buckling factor (λ) is the factor that scales an applied load (P) to cause buckling in the structure. Normally, a non-dimensional buckling factor (λ^*) is used, given as

$$\lambda^* = \lambda P \left(\frac{b^2}{c\, \pi^2 D} \right) \tag{11}$$

In this article, a subscript is attached the symbol of the non-dimensional buckling factor to indicate the applied load as follows: λ_ξ^* means only the uniaxial P_ξ is applied, λ_b^* means equal uniaxial loads P_ξ and P_η are applied, and λ_s^* means only the shear load $P_{\xi\eta}$ is applied.

2.4. Extended Kantorovich method (EKM)

The solution (w) is assumed as the summation of many terms, each is a multiplication of univariate functions of different variables. For the case of two dimensional plate, the solution may be approximated as

$$w(\xi,\eta) = \sum_{i=1}^{n} f_i(\xi) g_i(\eta) \tag{12}$$

where n is the number of terms, $f_i(\xi)$ and $g_i(\eta)$ are univariate functions. When the solution is assumed consisting of only one term, i.e. $(n = 1)$, then it is called the single-term EKM, otherwise it is called the multi-term EKM (MTEKM). Eq. (12) can be rewritten in matrix form as

$$w(\xi,\eta) = f\, g \tag{13}$$

where f is the single row matrix $\left[f_1(\xi), f_2(\xi), ..., f_n(\xi) \right]$, and g is the single column matrix $\left[g_1(\eta), g_2(\eta), ..., g_n(\eta) \right]^T$.

The EKM can be summarized as follows. At first, one part of the solution functions, f or g, is assumed. Assumed functions do not have to satisfy any of the boundary conditions. Then, the problem is solved for the other unknown group of functions. Next, using calculated functions, the problem is solved again for the first group of functions. This process is repeated until a satisfying convergence is achieved.

Two different problems have to be formulated, one for finding g with known f, and the second is for finding f with known g. For the sake of brevity, only the problem of finding g with known f is formulated here. Interested ones can formulate the second problem following the same steps shown in detail in the next section.

2.5. Governing equations and boundary conditions

In this section, the stability equation and boundary conditions are derived by implementing the principle of the minimum potential energy. This derivation starts with the substituting of the approximate solution of Eq. (13) in the transformed functional of the potential energy in Eq. (10), resulting in Eq. (14).

$$
\begin{aligned}
&e_p(f,g) = \\
&\frac{D}{2c^3}\iint\Big[(f''g)^2+(fg'')^2+2R_1(f''g)(fg'') \\
&\qquad -4s(f'g')\left(f''g+fg''\right)+2R_2(f'g')^2\Big]d\xi d\eta \\
&+\frac{1}{2}\iint\Big[k_n(fg)^2+\frac{k_p}{c}\Big((f'g)^2+(fg')^2 \\
&\qquad -2s(f'g)(fg')\Big)\Big]d\xi d\eta \\
&-\frac{1}{2}\iint\left[P_\xi(f'g)^2+P_\eta(fg')^2+2P_{\xi\eta}(f'g)(fg')\right]d\xi d\eta
\end{aligned}
\tag{14}
$$

Assuming all the functions in f are known, then the two-dimensional functional in Eq. (14) is reduced to an one-dimensional functional of the functions g as shown in Eq. (15).

$$
\begin{aligned}
&e_p(g) = \\
&\frac{D}{2c^3}\int\Big[(A_2g)^2+(A_0g'')^2+2R_1(A_2g)(A_0g'') \\
&\qquad -4s(A_1g')\left(A_2g+A_0g''\right)+2R_2(A_1g')^2\Big]d\eta \\
&+\frac{1}{2}\int\Big[\frac{k_p}{c}\left((A_1g)^2+(A_0g')^2-2s(A_1g)(A_0g')\right) \\
&\qquad +k_n(A_0g)^2\Big]d\eta \\
&-\frac{1}{2}\int\left[P_\xi(A_1g)^2+P_\eta(A_0g')^2+2P_{\xi\eta}(A_1g)(A_0g')\right]d\eta
\end{aligned}
\tag{15}
$$

where A_i is single row matrix $(1\times n)$, given by

$$
A_i=\int_{-a}^{+a}\left[\frac{d^if}{d\xi^i}\right]d\xi \tag{16}
$$

The functions g that make the energy functional stationary have to make its first variation vanish (Eisenberger and Alexandrov, 2003; Jones, 2006). The first variation, also known as the Gateaux derivative, of the one-dimensional functional of the potential energy presented in Eq. (15) is $\delta e_p(g,\delta_g)$ and obtained as

$$
\begin{aligned}
&\delta e_p(g,\delta_g)=0= \\
&\int_{-b}^{+b}\delta_g\Big[\frac{D}{c^3}\left(R_1\hat{A}_{(2,0)}g''+\hat{A}_{(2,2)}g-2s\hat{A}_{(2,1)}g'\right) \\
&\qquad +k_nc\hat{A}_{(0,0)}g+\frac{k_p}{c}\left(\hat{A}_{(1,1)}g-s\hat{A}_{(1,0)}g'\right) \\
&\qquad -P_\xi\hat{A}_{(1,1)}g-P_{\xi\eta}\hat{A}_{(1,0)}g'\Big]d\eta \\
&+\int_{-b}^{+b}\delta_g'\Big[\frac{D}{c^3}\left(-2R_2\hat{A}_{(1,1)}g'-2s\hat{A}_{(1,0)}g''-2s\hat{A}_{(1,2)}g\right) \\
&\qquad +\frac{k_p}{c}\left(\hat{A}_{(0,0)}g'-s\hat{A}_{(0,1)}g\right) \\
&\qquad -P_\eta\hat{A}_{(0,0)}g'-P_{\xi\eta}\hat{A}_{(0,1)}g\Big]d\eta \\
&+\int_{-b}^{+b}\delta_g''\Big[\frac{D}{c^3}\left(\hat{A}_{(0,0)}g''-2s\hat{A}_{(0,1)}g'+R_1\hat{A}_{(0,2)}g\right)\Big]d\eta
\end{aligned}
\tag{17}
$$

where $\hat{A}_{(i,j)}$ is $(n\times n)$ matrix given by

$$
\hat{A}_{(i,j)}=\int_{-a}^{+a}\left[\left[\frac{d^if}{d\xi^i}\right]^T\left[\frac{d^jf}{d\xi^j}\right]\right]d\xi \tag{18}
$$

Implementing the integration by parts on each integral contains derivatives of δ gives

$$
\begin{aligned}
&\delta e_p(g,\delta_g)=0= \\
&\int_{-b}^{+b}\left[T_1+T_{P1}\right]\delta_g d\eta+\delta_g\Big[T_2+T_{P2}\Big]_{-b}^{+b}+\delta_g'\Big[T_3\Big]_{-b}^{+b}
\end{aligned}
\tag{19}
$$

where T's are single column matrices $(n\times 1)$, obtained as

$$
\begin{aligned}
&T_1= \\
&\frac{D}{c^3}\Big(\hat{A}_{(0,0)}g''''+2sQ_{(1,0)}g'''-2sQ_{(2,1)}g'+\hat{A}_{(2,2)}g \\
&\qquad +\left(2R_2\hat{A}_{(1,1)}+R_1\left(\hat{A}_{(2,0)}+\hat{A}_{(0,2)}\right)\right)g''\Big) \\
&+k_nc\hat{A}_{(0,0)}g+\frac{k_p}{c}\left(\hat{A}_{(1,1)}g-sQ_{(1,0)}g'-\hat{A}_{(0,0)}g''\right) \\
&T_2=\frac{D}{c^3}\Big(-\hat{A}_{(0,0)}g'''-2sQ_{(1,0)}g'' \\
&\qquad -(2R_2\hat{A}_{(1,1)}+R_1\hat{A}_{(0,2)})g'-2s\hat{A}_{(1,2)}g\Big) \\
&+\frac{k_p}{c}\left(\hat{A}_{(0,0)}g'-s\hat{A}_{(0,1)}g\right) \\
&T_3=\frac{D}{c^3}\left(\hat{A}_{(0,0)}g''-2s\hat{A}_{(0,1)}g'+R_1\hat{A}_{(0,2)}g\right) \\
&T_{P1}=P_\eta\hat{A}_{(0,0)}g''-P_{\xi\eta}Q_{(1,0)}g'-P_\xi\hat{A}_{(1,1)}g \\
&T_{P2}=-P_{\xi\eta}\hat{A}_{(0,1)}g-P_\eta\hat{A}_{(0,0)}g'
\end{aligned}
\tag{20}
$$

where $Q_{(i,j)}$ is $(n\times n)$ matrix, given by

$$
Q_{(i,j)}=\hat{A}_{(i,j)}-\hat{A}_{(j,i)} \tag{21}
$$

Since δ_g is an arbitrary function, each of the three summed parts in Eq. (19) has to vanish. Equating the first part to zero produces n linear ordinary differential equations (ODE) that have to be satisfied through the interval $\{-b,+b\}$, i.e. the governing system of equations. In order to obtain a nontrivial solution, $[T_1+T_{P1}]$ has to vanish. So,

$$
T_1+T_{P1}=0 \tag{22}
$$

is the governing system of equations. Equating each of the later two parts to zero produces two systems of equations, each has n linear ODE's that have to be satisfied at the boundary points ($-b$ and $+b$), i.e. the boundary conditions, given as

$$
\begin{aligned}
&\text{either} \quad g=0 \quad \text{or} \quad T_2+T_{P2}=0 \\
&\text{and either} \quad g'=0 \quad \text{or} \quad T_3=0
\end{aligned}
\tag{23}
$$

To find the buckling factor λ, the governing equations in Eq. (22) are solved as a generalized eigenvalue problem, rewritten as

$$
T_1=-\lambda T_{P1} \tag{24}
$$

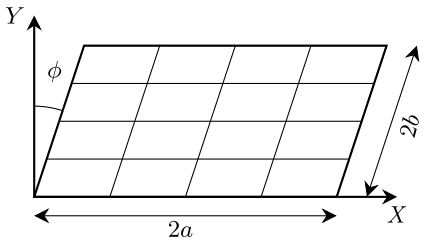

Fig. 4. A typical skew plate having coarse mesh of 4 elements per edge.

with the boundary conditions rewritten as

$$\text{either} \quad g = 0 \quad \text{or} \quad T_2 + \lambda T_{P2} = 0 \qquad (25)$$
$$\text{and either} \quad g' = 0 \quad \text{or} \quad T_3 = 0$$

Solving this generalized eigenvalue problem gives the buckling factor λ as the first eigenvalue, and n functions represent the obtained set of equations g.

Each edge of a plate can be either clamped (C) having $g = g' = 0$, simply supported (S) having $g = T_3 = 0$, or free (F) having $T_2 + \lambda T_{P2} = T_3 = 0$. The boundary conditions of a plate are described by stating the boundary condition of each edge in counterclockwise direction, starting from the left edge, as shown in Fig. 1, in which the labeling sequence is written beside the edges. For example, ($CSFC$) means that edge: $\xi = \{-a\}$ is clamped, edge: $\eta = \{-b\}$ is simply supported, edge: $\xi = \{+a\}$ is free and edge: $\eta = \{+b\}$ is clamped.

3. ANSYS finite element model

In addition to the analytical and numerical solutions found in the literature, EKM results are also compared to the those obtained using the finite element method (FEM). FEM is implemented using ANSYS® Mechanical APDL software. The plate is modeled using the SHELL281 layered shell elements. The elastic foundation is modeled with CONTA174 to TARGE170 bonded contact pair as described by SimuTech (2019). SURF153 elements are used to wrap each loaded edge. SURF153 elements provided the ability to simply apply pressure load in the (ξ, η) directions.

SHELL281 element provides accurate results for the buckling problem of thin plates (Hassan and Kurgan, 2019, 2020). The skew plate model is meshed as 100 elements which are found fine enough to obtain the converged results. Fig. 4 shows the meshing of the skew plate using smaller number of elements.

4. Numerical results and discussion

The derived generalized eigenvalue ODE problems in Eq. (24) with the boundary conditions in Eq. (25) are solved numerically using Chebfun, which is an open-source package of numerical computation, runs in the MATLAB environment (Driscoll et al., 2014). Chebfun provides a convenient way to express eigenvalue ODE problems and their boundary conditions. This section starts with a look at the convergence and then accuracy of the presented EKM. Then, a study of the effects of the different parameters on the buckling load is conducted.

4.1. EKM convergence

First, the simpler problem of SSSS rectangular plate under uniaxial compression P_ξ has been considered. The aspect ratio of the plate is chosen to be $a/b = 2$. Fig. 5 shows the obtained solution functions $g_j(\eta)$ and $f_i(\xi)$ through the first three iterations, started by a random function g_0 that did not necessarily satisfy any of the boundary conditions. Table 1 shows the obtained non-dimensional buckling factor λ^*_ξ at the end of each iteration for two runs with different initial trail

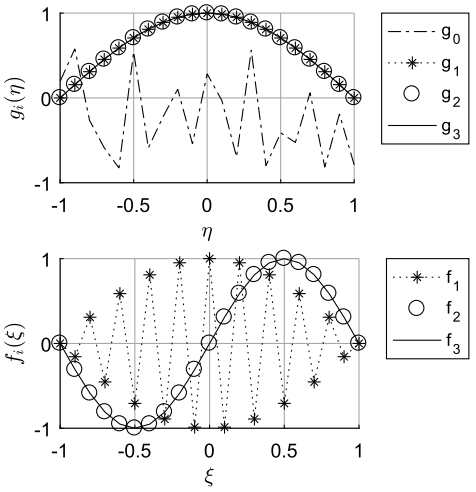

Fig. 5. $g_i(\eta)$ and $f_j(\xi)$ at end of each iteration starting from random $g_0(\eta)$.

Table 1
λ^* of SSSS square plate under uniaxial compression through EKM iterations.

$g_0(\eta)$	EKM iterations				Exact
	1	2	3	4	(Reddy, 2006)
Random	8.410502	3.99992	4.00000	4.00000	4
$g_0(\eta) = 1$	6.25000	4.00000	4.00000	–	

functions. The first run starts with a random function, while the second starts with a constant function: $g_0(\eta) = 1$. Fig. 5 along with Table 1 shows that even with a random trail function $g_0(\eta)$, the convergence of EKM is rapid. For all those presented results, the solution is considered converged once the difference $\triangle\lambda^*$ between the non-dimensional buckling factor of two successive iterations is less than 10^{-5}. For the case in hand, three iterations were enough for EKM to converge starting from a random trail function. Better the initial guess of $g_0(\eta)$ faster the convergence. An important point to note is that although the initial trail function does not have to satisfy any of the boundary conditions, using random initial $g_0(\eta)$ may sometimes make EKM not to converge. It is found better to guess a smooth initial function.

The convergence speed is found varying with the boundary conditions. Fig. 6 shows the convergence of the buckling solution for the same rectangular plate with various boundary conditions. Both clamped and free edges found increasing the required iterations starting from the same trial function $g_0(\eta) = 1$. It is obvious that if another trail function is used then the number of iterations required for each set of boundary conditions would probably change. The sole conclusion from this comparison is that different boundary conditions may require more or fewer iterations starting from the same initial trail function.

Another factor that affects the convergence speed is the skew angle ϕ. To examine its effect, SCSF rhombic plates, i.e. having aspect ratio $a/b = 1$, are considered. Results plotted in Fig. 7 show that using the same number of terms, plates with bigger skew angles require EKM to do more iterations to converge for the same boundary conditions starting from the same initial trail functions. The number of terms does not show any effect on the convergence speed, but hugely impacts the computational time, which increases exponentially with the number of terms.

4.2. EKM accuracy

To examine the quality of the EKM, the obtained results have been compared to those available in the literature and the finite element solution using ANSYS® Mechanical APDL software. The comparisons are done in a way that shows how each aspect of the problem affects the

Table 2
Comparison of nondimensional buckling factor λ_{ξ}^{*} of thin square plate under uniaxial compression loading, resting on elastic foundation with different boundary conditions.

Method	k_n^*, k_p^*	Boundary conditions							
		SSSS	SCSC	CSCS	SSSC	CCCC	SFSF	SCSF	SSSF
EKM	0,0	4.0000	7.6904	6.7432	5.7402	10.0968	0.9523	1.6525	1.4016
	1,0	5.0266	7.9479	7.4909	6.7668	10.7603	1.9789	2.6791	2.4282
	0,1	18.9151	20.7392	22.5557	19.7238	24.0490	11.1150	14.7849	14.1697
	1,1	19.1718	20.9898	22.7614	19.9775	24.2515	12.1416	15.6283	15.1963
Analytical (Thai et al., 2013)	0,0	4.0000	7.6912	6.7431	5.7402	–	0.9523	1.6525	1.4016
	1,0	5.0260	7.9478	7.4908	6.7668	–	1.9789	2.6791	2.4282
	0,1	18.9151	20.7345	22.5573	19.7210	–	11.1150	14.8063	14.1697
	1,1	19.1717	20.9911	22.7613	19.9776	–	12.1416	15.6287	15.1963
Finite strip method (Shahrestani et al., 2018)	0,0	4.0001	7.6989	6.7433	5.7414	10.0742	0.9523	1.6527	–
	1,0	5.0267	7.9555	7.4910	6.7679	10.7383	1.9790	2.6793	–
	0,1	18.9156	20.7698	22.5581	19.7352	24.0582	11.1151	14.8124	–
	1,1	19.1722	20.9917	22.7622	–	24.2460	–	–	–

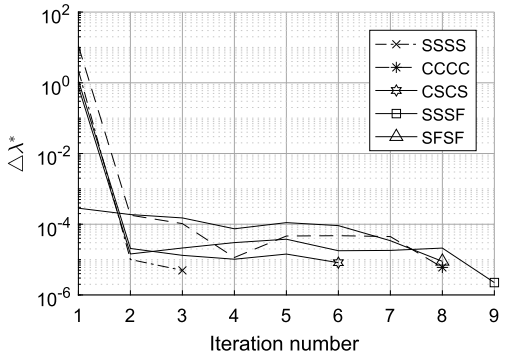

Fig. 6. Convergence of λ^* through EKM iterations for the case of rectangular plates with various boundary conditions under uniaxial compression.

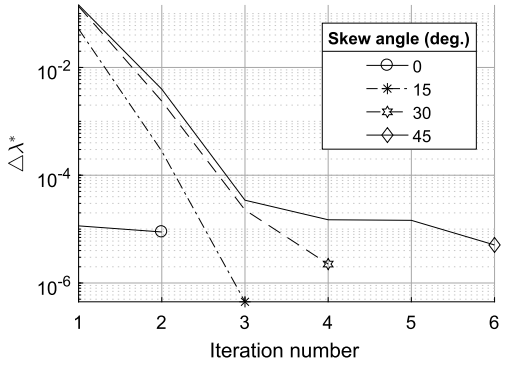

Fig. 7. Convergence of λ^* through EKM iterations for the case of $SSSS$ rhombic plates with various skew angles under uniaxial compression.

accuracy of EKM. These aspects are the boundary conditions, stiffness of the elastic foundation, aspect ratio, loading configuration, and the skew angle. Table 2 shows the non-dimensional buckling factors λ_{ξ}^{*} of a square isotropic plate under uniaxial compression for various boundary conditions and values of the elastic foundation parameters, obtained using the single-term EKM and compared with the analytical solutions of Thai et al. (2013) and the finite strip method solutions of Shahrestani et al. (2018). The single-term EKM is found accurate for the case of square plates with various boundary conditions. In addition, the results in Table 2 tell that introducing k_n^* and k_p^* of the elastic foundation to the buckling problem does not affect the accuracy of the results. This is also found true for the case of biaxial loading as Table 3 shows the perfect agreement between the EKM results and the analytical solutions of Lam et al. (2000) for various boundary conditions, proposing that

Table 3
λ_b^* of square plates resting on elastic foundation under equal biaxial compression obtained using EKM compared with the analytical solution of Lam et al. (2000).

k_n^*, k_p^*	Boundary conditions					
	SSSS		SCSC		SSSC	
	EKM	Analytical	EKM	Analytical	EKM	Analytical
0, 0	2.000	2.000	3.830	3.830	2.663	2.663
1, 0	2.513	2.513	4.280	4.280	3.132	3.132
0, 1	12.13	12.13	13.96	13.96	12.80	12.80
1, 1	12.65	12.65	14.41	14.41	13.26	13.26

Table 4
$\pi^2\lambda_{\xi}^{*}$ of rectangular plates with various aspect ratios a/b resting on elastic foundation obtained using EKM compared with the analytical solution of Akhavan et al. (2009).

a/b	k_n^*, k_p^*	Boundary conditions					
		SSSS		SCSC		SSSC	
		EKM	Analytical	EKM	Analytical	EKM	Analytical
0.5	0, 0	61.68	61.68	75.91	75.91	67.64	67.64
	1, 0.1	152.2	152.2	168.1	168.1	159.0	159.0
	10, 1	704.6	704.6	712.2	712.2	708.2	708.2
1	0, 0	39.48	39.48	75.91	75.91	56.65	56.65
	1, 0.1	69.61	69.61	91.37	91.36	82.90	82.90
	10, 1	212.0	212.0	230.0	230.0	220.0	220.0
2	0, 0	39.48	39.48	68.80	68.80	55.32	55.32
	1, 0.1	69.61	45.11	72.92	72.91	59.34	59.34
	10, 1	85.26	85.26	109.8	110.3	95.43	95.43

single-term EKM can be trusted for the cases of square plates under biaxial loading as well as the ones under uniaxial loading.

Obtained buckling shapes of the plate are also found to be correct as compared to the analytical solutions by Akhavan et al. (2009). For instance, the buckling shapes of SSSF square plates under uniaxial load P_y for various values of k_p^* obtained using EKM shown in Fig. 8 are the same as those presented in (Akhavan et al., 2009).

Table 4 shows that the single-term EKM is also accurate for different values of the aspect ratio a/b. From the comparisons presented above, it can be concluded that single-term EKM is an accurate method for buckling analysis of rectangular plates under uniaxial as well as biaxial loading with various boundary conditions, configurations of elastic foundation and aspect ratios.

The effect of the skew angle on the accuracy of the EKM is illustrated in Fig. 9, which shows the percentage relative difference (e) between the EKM results and the analytical solution of (Kitipornchai et al., 1993). The percentage relative difference is given as

$$e = \frac{(\lambda^*)_{\text{EKM}} - (\lambda^*)_{\text{ref.}}}{(\lambda^*)_{\text{ref.}}} \times 100\% \tag{26}$$

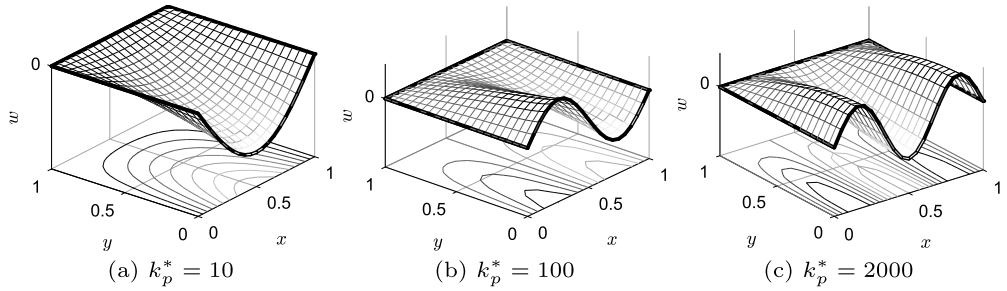

Fig. 8. Buckling shapes of uniaxially loaded $SSSF$ plate for range of k_p^*.

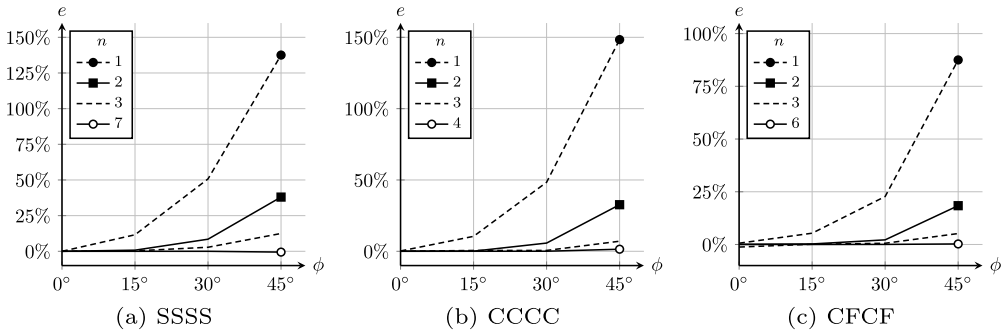

Fig. 9. Percentage relative difference e between λ_ξ^* obtained using EKM with various number of terms n and the analytical solution of Kitipornchai et al. (1993) for rhombic plates subject to uniaxial loads.

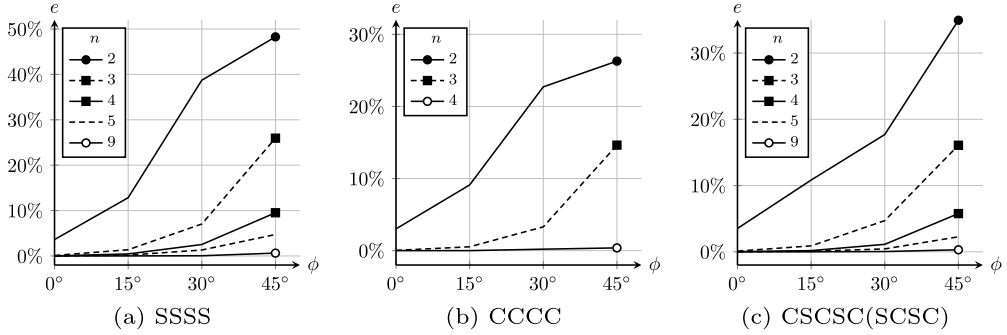

Fig. 10. Percentage relative difference e between λ_s^* obtained using EKM with various number of terms n and the DQM solution of Wang and Yuan (2018) for rhombic plates subject to shear loads.

Results show that, for the different types of boundary conditions, as the skew angle gets bigger, more terms are needed to obtain accurate results. EKM is found overestimating the λ^* more as the skew angle gets bigger. Different boundary conditions are found to need different numbers of terms to achieve the same accuracy. For instance, the 45° CCCC skew plate shown in Fig. 9b needs 4 terms, while the SSSS plate with the same skew angle shown in Fig. 9a needs 7 terms to achieve the same level of accuracy. Fig. 10 shows the same effect of the skew angle on the accuracy of the EKM results in the case of the shear loading $P_{\xi\eta}$ for different boundary conditions. The percentage relative difference e in Fig. 10 is between the EKM solutions and the DQM solutions of Wang and Yuan (2018).

From the results in Figs. 9 and 10, it comes clear that the single-term EKM is not suitable for the buckling analysis of the plates with a skew angle other than zero, under uniaxial or biaxial loading. Furthermore, the single-term EKM is not applicable to the problem of plate buckling under shear loading even for the rectangular plates. Using just a single term, i.e. $n = 1$, makes all the Q's in Eq. (19) vanish, which eliminates the $P_{\xi\eta}$ term from the governing equations.

Numerical results of buckling factor λ^* for the rhombic plates under uniaxial loading are shown in Tables 5 and 6, and those for the cases of biaxial and shear loading are shown in Table 7 compared to solutions found in the literature. The numbers of EKM terms are given as superscripts after the EKM results.

Tables 5 and 6 show also the non-dimensional buckling factor λ_ξ^* for skew plates with various aspect ratios. Those results show that the aspect ratio a/b of the plate does not have any effect on the accuracy of the EKM. Including more terms is found to provide better results, but at the expense of the computational time.

4.3. Effects of the skew angle, aspect ratio and elastic foundation on the buckling factor

Fig. 11 is a set of logarithmic plots that show the effect of the aspect ratio a/b and the skew angle ϕ on the nondimensional buckling factor λ^* of a skew SSSS plate under uniaxial, biaxial and shear loading. In the case of the uniaxial loading, Fig. 11a shows that increasing the aspect ratio quickly drops the buckling factor λ_ξ^* when a/b is less than 1, then it gets fluctuating less and less as the aspect ratio gets bigger. Buckling factor λ_ξ^* is found increasing as the skew angle ϕ gets bigger. Also, it is can be seen that the effect of the skew angle gets smaller as the aspect ratio gets bigger. The effect of increasing the skew angle gets larger as the skew angle does. For instance, the difference in λ^* between the

Table 5
λ_{ξ}^{*} of skew plates with various aspect ratios, skew angles and boundary conditions under uniaxial load obtained using EKM compared with the DQM solution of Wang and Yuan (2018), the analytical solution of Kitipornchai et al. (1993), and the FEM solution of ANSYS.

a/b	Method	BC							
		SSSS				CCCC			
		$\phi = 0°$	15°	30°	45°	0°	15°	30°	45°
$\frac{1}{2}$	EKM	6.2500^{1}	6.9835^{4}	9.9159^{7}	19.1321^{7}	19.3388^{2}	21.5551^{4}	30.295^{4}	54.515^{7}
	Analytical	6.2499	6.9782	9.9166	19.2473	19.3377	21.5540	30.2876	54.5553
	DQM	6.2500	6.9965	9.8787	18.859	19.339	21.555	30.289	54.539
	FEM	6.1886	6.9001	9.7394	18.6225	19.2425	21.3469	29.3619	49.7263
1	EKM	4.0000^{1}	4.3985^{4}	5.8902^{7}	10.0455^{7}	10.0753^{2}	10.8344^{4}	13.539^{7}	20.109^{7}
	Analytical	4.0000	4.3938	5.8969	10.1032	10.0738	10.8345	13.5377	20.1115
	DQM	4.0000	4.3919	5.8716	10.006	10.074	10.835	13.538	20.105
	FEM	3.9626	4.3439	5.7576	9.4302	10.0520	10.8057	13.4656	19.7801
$\frac{3}{2}$	EKM	4.3403^{1}	4.6822^{4}	5.9218^{6}	9.1427^{7}	8.3523^{2}	8.9345^{4}	11.030^{7}	16.267^{7}
	Analytical	4.3403	4.6783	5.9226	9.1658	8.3504	8.9333	11.0296	16.2603
	DQM	4.3403	4.6770	5.9019	8.9974	8.3505	8.9335	10.9843	16.258
	FEM	4.3075	4.6373	5.8293	8.8080	8.3330	8.9107	10.984	16.1386
2	EKM	4.0000^{1}	4.3446^{4}	5.6112^{7}	8.8757^{7}	7.8673^{2}	8.3866^{4}	10.455^{7}	15.154^{7}
	Analytical	4.0000	4.3417	5.6206	8.9046	7.8670	8.3866	10.2834	15.1971
	DQM	4.0000	4.3400	5.5933	8.7691	7.8671	8.3867	10.283	15.157
	FEM	3.9712	4.3050	5.5341	8.6909	7.8507	8.3662	10.2462	15.0791
$\frac{5}{2}$	EKM	4.1344^{1}	4.4378^{4}	5.5432^{7}	8.4614^{7}	7.5732^{2}	8.1243^{4}	9.878^{7}	14.890^{7}
	Analytical	4.1344	4.4365	5.5556	8.5024	7.5731	8.1151	9.9700	14.9399
	DQM	4.1344	4.4349	5.5301	8.3109	7.5731	8.1275	9.9476	14.788
	FEM	4.1068	4.4025	5.4281	8.2923	7.5584	8.0977	9.9154	14.6274

Note: The superscripts indicate the number of the EKM terms (n).

Table 6
$\lambda_{x}^{*}i$ of skew plates with various aspect ratios, skew angles and boundary conditions under uniaxial load obtained using EKM compared with the analytical solution of Kitipornchai et al. (1993) and the FEM solution of ANSYS.

a/b	Method	BC							
		SFSF				CFCF			
		$\phi = 0°$	15°	30°	45°	0°	15°	30°	45°
$\frac{1}{2}$	EKM	3.8926^{1}	4.4098^{4}	6.4535^{6}	11.7152^{5}	15.8285^{2}	17.6475^{4}	23.4382^{6}	34.0955^{6}
	Analytical	3.8926	4.4093	6.4561	11.7162	15.8221	17.6435	23.4293	34.0985
	FEM	3.8840	4.3929	6.3861	11.2259	15.7349	17.4335	22.6297	31.2363
1	EKM	0.9523^{1}	1.0677^{4}	1.5140^{6}	2.7806^{5}	3.9208^{2}	4.2844^{4}	5.6171^{6}	8.118^{6}
	Analytical	0.9523	1.0674	1.5128	2.7443	3.9193	4.2824	5.6159	8.0948
	FEM	0.9512	1.0650	1.5027	2.6928	3.9115	4.2593	5.5142	7.7364
$\frac{3}{2}$	EKM	0.4168^{1}	0.4634^{4}	0.6399^{6}	1.1176^{5}	1.7302^{2}	1.8540^{4}	2.2833^{6}	3.2441^{6}
	Analytical	0.4168	0.4633	0.6384	1.1080	1.7287	1.8528	2.2826	3.2347
	FEM	0.41654	0.4625	0.6351	1.0915	1.7264	1.8458	2.2528	3.1121
2	EKM	0.2322^{1}	0.2567^{4}	0.3459^{6}	0.5808^{5}	0.9668^{2}	1.0212^{4}	1.1973^{6}	1.5376^{6}
	Analytical	0.2322	0.2566	0.3464	0.5749	0.9663	1.0205	1.1971	1.5375
	FEM	0.2321	0.2563	0.3449	0.5673	0.9652	1.0174	1.1848	1.4926
$\frac{5}{2}$	EKM	0.1477^{1}	0.1627^{4}	0.2152^{6}	0.3526^{5}	0.6160^{2}	0.6431^{4}	0.7285^{6}	0.8826^{6}
	Analytical	0.1477	0.1626	0.2165	0.3478	0.6151	0.6428	0.7293	0.8827
	FEM	0.1477	0.1624	0.2156	0.34361	0.6144	0.6411	0.7231	0.8618

Note: The superscripts indicate the number of the EKM terms (n).

Table 7
Nondimensional biaxial λ_{b}^{*} and shear λ_{s}^{*} buckling factors of rhombic plates with various skew angles and boundary conditions obtained using EKM compared with the DQM solution of Wang and Yuan (2018).

$\phi°$	Method	BC									
		SSSS		CCCC		SCSC(CSCS)		SFSF(FSFS)		CFCF(FCFC)	
		λ_{b}^{*}	λ_{s}^{*}	λ_{b}^{*}	λ_{s}^{*}	λ_{b}^{*}	λ_{s}^{*}	λ_{b}^{*}	λ_{s}^{*}	λ_{b}^{*}	λ_{s}^{*}
0	EKM	2.0000^{1}	9.3256^{4}	5.3038^{2}	14.6476^{3}	3.8299^{1}	12.5573^{5}	0.9322^{1}	4.2327^{4}	2.7662^{1}	7.463^{4}
	DQM	2.0000	9.3245	5.3036	14.642	3.8299	12.565	0.9322	4.2303	2.7423	7.4860
15	EKM	2.2028^{4}	7.1017^{4}	5.7151^{3}	11.4051^{4}	4.1801^{4}	9.7665^{5}	1.0357^{4}	3.3222^{5}	2.8530^{5}	5.6790^{5}
	DQM	2.1966	7.0701	5.7150	11.406	4.1808	9.7594	1.0361	3.3201	2.8504	5.6816
30	EKM	2.9498^{7}	6.6481^{7}	7.1650^{4}	10.8958^{5}	5.4544^{7}	9.3138^{7}	1.3117^{7}	2.910^{6}	3.2598^{5}	5.1370^{6}
	DQM	2.9394	6.6186	7.1603	10.887	5.4515	9.3053	1.3097	2.9058	3.2542	5.1314
45	EKM	4.9981^{8}	7.9754^{9}	10.5896^{6}	13.0729^{6}	8.5138^{8}	11.2549^{7}	1.6247^{4}	3.1045^{6}	4.3057^{7}	5.681^{7}
	DQM	4.9517	7.9221	10.575	13.087	8.5280	11.184	1.6151	3.0582	4.2802	5.6422

Note: The superscripts indicate the number of the EKM terms (n).

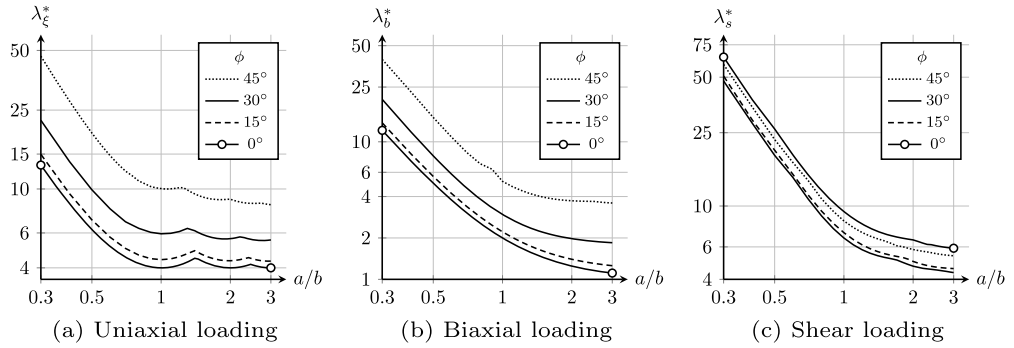

Fig. 11. Non-dimensional buckling factor λ^* of SSSS plate for a range of aspect ratios a/b and skew angles ϕ under different types of loading.

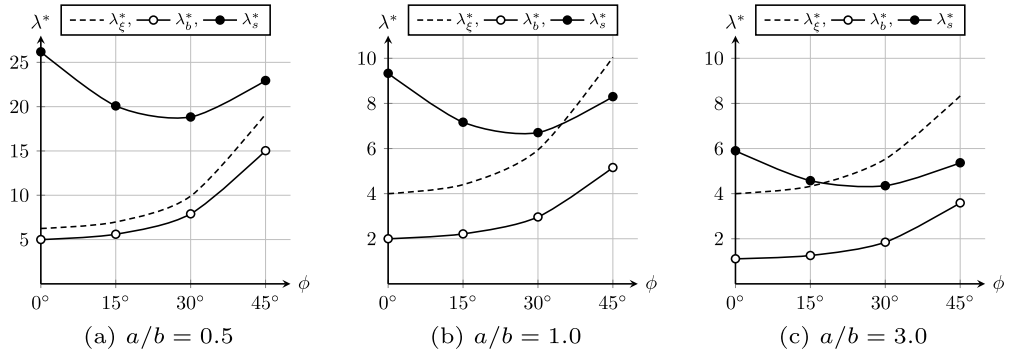

Fig. 12. Comparison of the non-dimensional buckling factor λ^* of SSSS plate for a range of skew angles ϕ under different types of loading at different values of aspect ratio a/b.

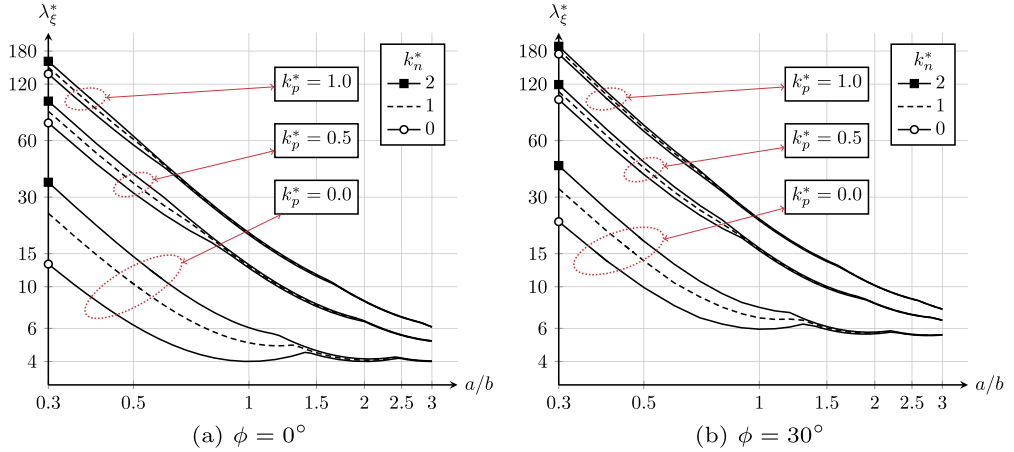

Fig. 13. Non-dimensional buckling factor λ_ξ^* of (a) rectangular and (b) skew SSSS plate with a range of aspect ratios a/b under uniaxial loading resting on the Pasternak elastic foundation.

cases $\phi = 30$ and $\phi = 45$ is much bigger than the difference between the cases $\phi = 30$ and $\phi = 15$.

The same effects are also seen in the case of the biaxial loading in Fig. 11b.

For the shear loading case, the aspect ratio a/b has the same effect on the buckling factor λ_s^* as the cases of the uniaxial and biaxial loading, as shown in Fig. 11c. However, the effect of the skew angle is different in this case. To track the effect of the skew angle on the buckling factor λ_s^*, snapshots are taken from the plots in Fig. 11 at some different aspect ratios and shown in Fig. 12. These plots show clearly the different effect of the skew angle ϕ on the buckling factor λ_s^* as compared to λ_ξ^* and λ_b^*. Fig. 12 also shows that as the aspect ratio gets bigger the buckling factors drop and the effect of the skew angle gets smaller. Lastly, the effect of the elastic foundation stiffness on the buckling factor is illustrated by the logarithmic plots in Fig. 13, which show the buckling factor λ_ξ^* of SSSS rectangular and skew plates under uniaxial loading for a range of aspect ratios resting of the Pasternak elastic foundation with different values of stiffness. The plots show that both k_n^* and k_p^* increase the buckling factor. However, it can be seen clearly that as the aspect ratio gets bigger, the effect of the shear stiffness k_p^* decreases, and the effect of the normal stiffness k_n^* vanishes. The same effects are also observed for the case of biaxial loading as shown in Fig. 14a, and the case of shear loading as shown in Fig. 14b. These effects are not exclusive to the buckling factor of SSSS plates. For example, as Fig. 15 shows, the same effects are seen in the case of the CCCC rectangular plate.

5. Conclusion

The extended Kantorovich method (EKM) is successfully implemented to solve the buckling problem of the skew plate for the first

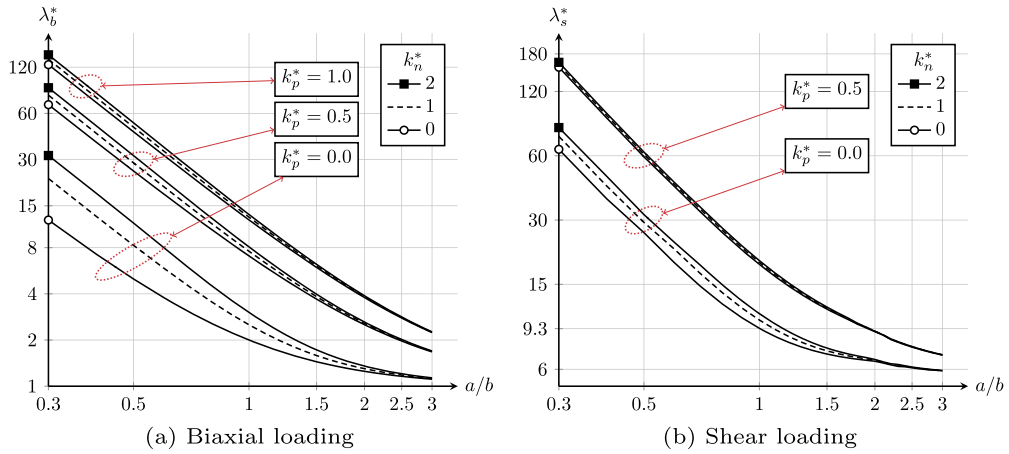

Fig. 14. Non-dimensional buckling factor λ^* of a rectangular SSSS plate with a range of aspect ratios a/b under (a) biaxial and (b) shear loading resting on the Pasternak elastic foundation.

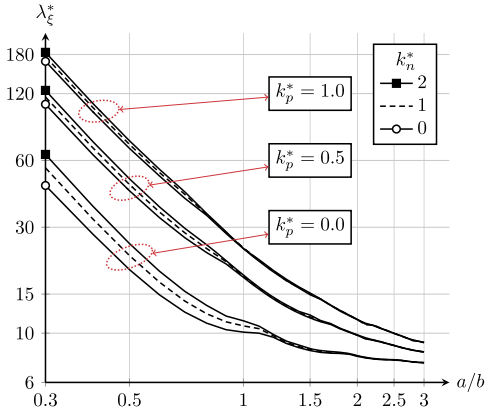

Fig. 15. Non-dimensional buckling factor λ_ξ^* of a rectangular CCCC plate with a range of aspect ratios a/b under uniaxial loading resting on the Pasternak elastic foundation.

time. Accuracy and convergence of the EKM are investigated. Stability equations and boundary conditions terms are derived from the principle of the minimum total potential energy using the variational calculus and expressed in an oblique coordinate system. The skew plate is assumed thin and the classical plate theory CPT is used as the base formulation. Chebfun numerical computation package is used to solve the generalized eigenvalue problem. The plate is assumed to be resting on the Pasternak elastic foundation and is under in-plane loading. Uniaxial and biaxial uniform compression and shear loads are considered. Various boundary conditions are implemented. The convergence of EKM is examined and found rapid even when starting by random initial trail function. Accuracy of the method is evaluated by comparing obtained results with those found in the literature and to the finite element solution using ANSYS.

The single-term EKM is found to be accurate in buckling analysis of thin rectangular plates under in-plane uniform uniaxial and biaxial compression resting on an elastic foundation; but not reliable in the case of skew plates, as it tends to considerably overestimate the buckling load. The single-term EKM is also found not applicable for the buckling analysis of plates under shear loading, so, the multi-term EKM has to be implemented for this analysis. Using the multi-term EKM is found accurate in the buckling analysis of the thin skew plates with various boundary conditions under different types of loading resting on the Pasternak elastic foundation. Results get better as more terms are used. Different problems require different numbers of terms to achieve the same level of accuracy. Using EKM in buckling analysis of thin skew plates is found simple, accurate, and rapid to converge. Lastly, the effects of the skew angle, aspect ratio, and elastic foundation stiffness on the buckling load are investigated and illustrated in figures.

Declarations

Author contribution statement

Ahmed Hassan Ahmed Hassan: Performed the experiments; Analyzed and interpreted the data; Contributed reagents, materials, analysis tools or data; Wrote the paper.

Naci Kurgan: Conceived and designed the experiments; Analyzed and interpreted the data; Contributed reagents, materials, analysis tools or data.

Funding statement

This research did not receive any specific grant from funding agencies in the public, commercial, or not-for-profit sectors.

Competing interest statement

The authors declare no conflict of interest.

References

Akhavan, H., Hashemi, S.H., Taher, H.R.D., Alibeigloo, A., Vahabi, S., 2009. Exact solutions for rectangular Mindlin plates under in-plane loads resting on Pasternak elastic foundation. Part I: buckling analysis. Comput. Mater. Sci. 44 (3), 968–978.

Chen, P.C., 1972. Buckling analysis of a rectangular plate by the Kantorovich method. Int. J. Mech. Sci. 14 (1), 15–24.

Driscoll, T.A., Hale, N., Trefethen, L.N., 2014. Chebfun Guide. Pafnuty Publications. http://www.chebfun.org/docs/guide/.

Eisenberger, M., Alexandrov, A., 2003. Buckling loads of variable thickness thin isotropic plates. Thin-Walled Struct. 41 (9), 871–889.

Eisenberger, M., Shufrin, I., 2009. Buckling of plates by the multi term extended Kantorovich method. In: Proceedings of the 7th EUROMECH Solid Mechanics Conference. Lisbon, Portugal.

Gadade, A.M., Lal, A., Singh, B., 2020. Stochastic buckling and progressive failure of layered composite plate with random material properties under hygro-thermo-mechanical loading. Mater. Today Commun. 22, 100824.

Grimm, T., Gerdeen, J., 1975. Instability analysis of thin rectangular plates using the Kantorovich method. J. Appl. Mech. 42 (1), 110–114.

Hassan, A.H.A., Kurgan, N., 2019. Modeling and buckling analysis of rectangular plates in ansys. Int. J. Eng. Appl. Sci. 11 (1), 310–329.

Hassan, A.H.A., Kurgan, N., 2020. Bending analysis of thin fgm skew plate resting on Winkler elastic foundation using multi-term extended Kantorovich method. Int. J. Eng. Sci. Technol.

Jaberzadeh, E., Azhari, M., Boroomand, B., 2013. Inelastic buckling of skew and rhombic thin thickness-tapered plates with and without intermediate supports using the element-free Galerkin method. Appl. Math. Model. 37 (10–11), 6838–6854.

Jaunky, N., Knight, N., Ambur, D., 1995. Buckling of arbitrary quadrilateral anisotropic plates. AIAA J. 33 (5), 938–944.

Jones, R.M., 2006. Buckling of Bars, Plates, and Shells. Bull Ridge Corporation.
Joodaky, A., Joodaky, I., 2015. A semi-analytical study on static behavior of thin skew plates on Winkler and Pasternak foundations. Int. J. Mech. Sci. 100, 322–327.
Joodaky, A., Kargarnovin, M.H., Mehrabadi, S.J., Barati, A.H.N., 2012. Bending and deflection analysis of thin fgm skew plates using extended Kantorovich method. Am. J. Sci. Res. 46, 67–78.
Joodaky, A., Joodaky, I., Hedayati, M., Masoomi, R., Farahani, E.B., 2013. Deflection and stress analysis of thin fgm skew plates on Winkler foundation with various boundary conditions using extended Kantorovich method. Composites, Part B, Eng. 51, 191–196.
Kargarnovin, M., Joodaky, A., Mehrabadi, S.J., 2010. Bending analysis of thin skew plates using extended Kantorovich method. ASME Paper No ESDA2010-24138.
Kennedy, J., Prabhakara, M., 1978. Buckling of simply supported orthotropic skew plates. Aeronaut. Q. 29 (3), 161–174.
Kerr, A.D., 1968. An extension of the Kantorovich method. Q. Appl. Math. 26 (2), 219–229.
Kerr, A.D., 1969. An extended Kantorovich method for the solution of eigenvalue problems. Int. J. Solids Struct. 5 (6), 559–572.
Kerr, A.D., Alexander, H., 1968. An application of the extended Kantorovich method to the stress analysis of a clamped rectangular plate. Acta Mech. 6 (2–3), 180–196.
Kitipornchai, S., Xiang, Y., Wang, C., Liew, K., 1993. Buckling of thick skew plates. Int. J. Numer. Methods Eng. 36 (8), 1299–1310.
Kitipornchai, S., Chen, D., Yang, J., 2017. Free vibration and elastic buckling of functionally graded porous beams reinforced by graphene platelets. Mater. Des. 116, 656–665.
Lam, K., Wang, C., He, X., 2000. Canonical exact solutions for Levy-plates on two-parameter foundation using Green's functions. Eng. Struct. 22 (4), 364–378.
Lopatin, A., Morozov, E., 2013. Buckling of a uniformly compressed rectangular sscf composite sandwich plate. Compos. Struct. 105, 108–115.
Mahmoudi, A., Benyoucef, S., Tounsi, A., Benachour, A., Adda Bedia, E.A., Mahmoud, S, 2017. A refined quasi-3d shear deformation theory for thermo-mechanical behavior of functionally graded sandwich plates on elastic foundations. J. Sandw. Struct. Mater.
Manickam, G., Bharath, A., Das, A.N., Chandra, A., Barua, P., 2018. Thermal buckling behaviour of variable stiffness laminated composite plates. Mater. Today Commun. 16, 142–151.
Mizusawa, T., Kajita, T., Naruoka, M., 1980. Analysis of skew plate problems with various constraints. J. Sound Vib. 73 (4), 575–584.
MonroeAerospacecom, 2019. Why do airplanes have swept wings. Tech. Rep. Monroe Aerospace. https://monroeaerospace.com/blog/why-do-airplanes-have-swept-wings/.
Rajabi, J., Mohammadimehr, M., 2019. Bending analysis of a micro sandwich skew plate using extended Kantorovich method based on Eshelby-Mori-Tanaka approach. Comput. Concr. 23 (5), 361–376.
Reddy, J.N., 2006. Theory and Analysis of Elastic Plates and Shells. CRC Press.
Saadatpour, M., Azhari, M., Bradford, M., 1998. Buckling of arbitrary quadrilateral plates with intermediate supports using the Galerkin method. Comput. Methods Appl. Mech. Eng. 164 (3–4), 297–306.
Shahrestani, M.G., Azhari, M., Foroughi, H., 2018. Elastic and inelastic buckling of square and skew fgm plates with cutout resting on elastic foundation using isoparametric spline finite strip method. Acta Mech. 229 (5), 2079–2096.
Shahsavari, D., Shahsavari, M., Li, L., Karami, B., 2018. A novel quasi-3d hyperbolic theory for free vibration of fg plates with porosities resting on Winkler/Pasternak/Kerr foundation. Aerosp. Sci. Technol. 72, 134–149.
Shufrin, I., Eisenberger, M., 2005a. Stability and vibration of shear deformable plates—first order and higher order analyses. Int. J. Solids Struct. 42 (3–4), 1225–1251.
Shufrin, I., Eisenberger, M., 2005b. Stability of variable thickness shear deformable plates—first order and high order analyses. Thin-Walled Struct. 43 (2), 189–207.
Shufrin, I., Eisenberger, M., 2006. Buckling of plates with variable in-plane forces. In: Analysis and Design of Plated Structures. Elsevier, pp. 26–55.
Shufrin, I., Eisenberger, M., 2007. Shear buckling of thin plates with constant in-plane stresses. Int. J. Struct. Stab. Dyn. 7 (02), 179–192.
Shufrin, I., Rabinovitch, O., Eisenberger, M., 2008a. Buckling of laminated plates with general boundary conditions under combined compression, tension, and shear—a semi-analytical solution. Thin-Walled Struct. 46 (7–9), 925–938.
Shufrin, I., Rabinovitch, O., Eisenberger, M., 2008b. Buckling of symmetrically laminated rectangular plates with general boundary conditions–a semi analytical approach. Compos. Struct. 82 (4), 521–531.
Shufrin, I., Rabinovitch, O., Eisenberger, M., 2009. Elastic nonlinear stability analysis of thin rectangular plates through a semi-analytical approach. Int. J. Solids Struct. 46 (10), 2075–2092.
Shufrin, I., Rabinovitch, O., Eisenberger, M., 2010. A semi-analytical approach for the geometrically nonlinear analysis of trapezoidal plates. Int. J. Mech. Sci. 52 (12), 1588–1596.
SimuTech, 2019. A Normal and Tangential Elastic Foundation in Workbench Mechanical. Tech. Rep. SimuTech Group. https://www.simutechgroup.com/tips-and-tricks/fea-articles/143-a-normal-and-tangential-elastic-foundation-in-workbench-mechanical.
Singhatanadgid, P., Jommalai, P., 2016. Buckling analysis of laminated plates using the extended Kantorovich method and a system of first-order differential equations. J. Mech. Sci. Technol. 30 (5), 2121–2131.
Singhatanadgid, P., Singhanart, T., 2019. The Kantorovich method applied to bending, buckling, vibration, and 3d stress analyses of plates: a literature review. Mech. Adv. Mat. Struct. 26 (2), 170–188.
Srinivasa, C., Kumar, Y.S.W.P., Banagar, A.R., 2018. Bending behavior of simply supported skew plates. Int. J. Sci. Eng. Res. 9, 21–26.
Thai, H.T., Park, M., Choi, D.H., 2013. A simple refined theory for bending, buckling, and vibration of thick plates resting on elastic foundation. Int. J. Mech. Sci. 73, 40–52.
Ungbhakorn, V., Singhatanadgid, P., 2006. Buckling analysis of symmetrically laminated composite plates by the extended Kantorovich method. Compos. Struct. 73 (1), 120–128.
Ventsel, E., Krauthammer, T., 2001. Thin Plates and Shells: Theory: Analysis, and Applications. CRC Press.
Wang, X., Yuan, Z., 2018. Buckling analysis of isotropic skew plates under general in-plane loads by the modified differential quadrature method. Appl. Math. Model. 56, 83–95.
Wu, H., Kitipornchai, S., Yang, J., 2017. Thermal buckling and postbuckling of functionally graded graphene nanocomposite plates. Mater. Des. 132, 430–441.
Xie, W.C., Elishakoff, I., 2000. Buckling mode localization in rib-stiffened plates with misplaced stiffeners–Kantorovich approach. Chaos Solitons Fractals 11 (10), 1559–1574.
Yu, T., Zhang, L., 1986. The elastic wrinkling of an annular plate under uniform tension on its inner edge. Int. J. Mech. Sci. 28 (11), 729–737.
Yuan, S., Jin, Y., 1998. Computation of elastic buckling loads of rectangular thin plates using the extended Kantorovich method. Comput. Struct. 66 (6), 861–867.
Zhang, L., Yu, T., 1988. The plastic wrinkling of an annular plate under uniform tension on its inner edge. Int. J. Solids Struct. 24 (5), 497–503.